International Journal of Quantum Information
(2026) 2640004 (18 pages)

DOI: 10.1142/S0219749926400046

World Scientific
www.worldscientific.com

Non-Markovianity in the Adapted Caldeira–Leggett Model

Luciano Manara

Istituto Nazionale di Fisica Nucleare
Sezione di Milano, Via Celoria 16, I-20133 Milan, Italy
luciano.manara@mi.infn.it

Andrea Smirne * and Bassano Vacchini †

Università degli Studi di Milano, Dipartimento
di Fisica, Via Celoria 16, I-20133 Milan, Italy

Istituto Nazionale di Fisica Nucleare, Sezione
di Milano, Via Celoria 16, I-20133 Milan, Italy
*andrea.smirne@unimi.it
†bassano.vacchini@mi.infn.it

Received 10 February 2026
Accepted 24 March 2026
Published 28 April 2026

We investigate the non-Markovian features of the Adapted Caldeira–Leggett model, a computationally efficient framework recently proposed to capture the essential physics of the standard Caldeira–Leggett model. While this effective model has been previously validated for decoherence and einselection, its ability to reproduce memory effects remains to be explored. By exploiting the model's capability to explicitly track both system and environment degrees of freedom, we provide a detailed characterization of non-Markovianity through the lens of information backflow. We evaluate the buildup of system-environment correlations and the corresponding modifications of the environmental state, assessing a quantitative upper bound for the revival of distinguishability in the reduced dynamics. Our results, obtained by comparing different distinguishability quantifiers such as trace distance and the square root of the Jensen–Shannon divergence, show that while correlations are primarily sensitive to coupling strength, environmental state changes are more heavily influenced by temperature. Our analysis substantiates the physical interpretation of the distinguishability-based approach to non-Markovianity, and confirms this variant of the Caldeira–Leggett model as a reliable tool for exploring the microscopic origins of different fundamental phenomena in quantum mechanics.

Keywords: Open quantum systems; Caldeira–Leggett model; non-Markovian dynamics.

1. Introduction

In most physical scenarios, the primary interest lies in studying the reduced degrees of freedom of a system while accounting for environmental influences through an

†Corresponding author.

effective description.[1–3] Indeed, an exact treatment of all environmental degrees of freedom is often computationally prohibitive, making such effective approaches a necessity.

However, certain situations demand detailed information about the surroundings to ensure a correct physical interpretation. A prominent example is the framework of Quantum Darwinism,[4–9] which seeks to explain the emergence of objective classical properties in the quantum evolution through the interaction between a system and its environment. Furthermore, the study of decoherence and its connection to einselection (environment-induced superselection) provides another fundamental case[5,10–14]; here, suitable pointer states emerge from the system-environment interaction, leading to classical behavior for specific observables.

Another crucial case arises in the investigation of memory effects in the reduced dynamics,[15–19] which is the core focus of this paper. Gaining access to the environmental degrees of freedom allows for an exploration of memory effects as arising from information backflow from the bath to the system, as suggested by the Breuer–Laine–Piilo approach to non-Markovianity.[20]

Given the challenge of tracking all involved degrees of freedom, even numerically, a new effective model has recently been proposed to capture the essential physics of the Caldeira–Leggett[21] model while remaining numerically efficient. This Adapted Caldeira–Leggett (ACL) model was introduced by Albrecht and coworkers.[22] While its validity has been demonstrated regarding decoherence and einselection,[22,23] this work aims to investigate whether the ACL model reliably describes non-Markovian features as well.

Our objective is threefold. First, we test the validity of the ACL model in reproducing a key physical property of the original Caldeira–Leggett framework: the non-Markovianity of the associated reduced dynamics. Second, we exploit the ACL model to investigate the actual information backflow, providing a deeper physical interpretation of the non-Markovian dynamics. Such an analysis has previously been unfeasible due to the aforementioned computational difficulties. Our results provide new insights into the origin of memory effects in the Caldeira–Leggett model and their dependence on the physical parameters characterizing the environment. Finally, we compare the performance of two distinguishability quantifiers, namely trace distance and square root of the Jensen–Shannon divergence, that have proven to have very close performances in the quantification of non-Markovianity, in estimating the information backflow.

The remainder of the paper is organized as follows. In Sec. 2, we introduce the ACL model, clarifying the details and relevant figures of merit used in environmental modeling. In Sec. 3, we introduce the adopted definition of non-Markovian dynamics, alongside its suggested physical interpretation and the quantities required to validate this perspective. Section 4 details our results for non-Markovianity within the model, benchmarking them against previous work; here, we also discuss the behavior of information backflow and its connection to the establishment of correlations and the system's influence on the environment. We further compare the

behavior of trace distance and square root of the Jensen–Shannon divergence in estimating the information backflow. Finally, in Sec. 5, we summarize our results and outline potential future developments.

2. Adapted Caldeira–Leggett Model

The ACL model is a fictitious model of system-environment interaction, designed to describe the dynamics of a continuous variable system interacting with a bosonic environment via position coupling. The model was introduced by Albrecht and coworkers in Ref. 22, where its effectiveness in describing decoherence and einselection was investigated, and was further studied with respect to its capability to describe equilibration and thermalization in Ref. 24. It arises as an *adaptation* of the well-known Caldeira–Leggett model[21,25,26] to make it more amenable to numerical analysis. In particular, this model lends itself to an analysis of the time evolution of all involved degrees of freedom, which is an essential ingredient for assessing certain physical features.

In this work, relying on the promising results obtained from the model for the description of the above-mentioned features, we will explore its validity in describing the non-Markovianity of the reduced system dynamics, as well as its interplay with the establishment of correlations between the system and the environment and the feedback of the system on the environment.

2.1. *System and environment modeling*

The ACL model is based on a Hamiltonian of the form

$$H = H_S \otimes 1_E + 1_S \otimes H_E + \gamma\, q_S \otimes X_E, \tag{1}$$

where the subscripts S and E denote operators acting on the system and environment degrees of freedom, respectively. The peculiarity of the model relies on two main ingredients. On the one hand, the system position operator q_S is constructed as a linear combination of creation and annihilation operators of a truncated harmonic oscillator. On the other hand, no specific microscopic structure is assumed for the environmental Hamiltonian H_E and for the environmental operator X_E appearing in the interaction term, which are instead modeled as Hermitian random matrices. As a consequence, both the system and the environment are described within finite-dimensional Hilbert spaces.

The finite dimensionality of the system degrees of freedom is obtained by defining a truncated annihilation operator a_S as

$$\langle n|a_S|m\rangle = \sqrt{m}\,\delta_{n,m-1}, \quad n \in \{0,\dots,N_S-1\}; \quad m \in \{1,\dots,N_S\}, \tag{2}$$

where N_S fixes the dimension of the truncated Hilbert space. By considering the adjoint operator $a_S^\dagger$, we define their linear combination

$$q_S = \frac{1}{\sqrt{2}}(a_S + a_S^\dagger) \tag{3}$$

as the dimensionless position operator of the system. We note that the definition in Eq. (2) implies modified commutation relations,

$$[a_S, a_S^\dagger] = 1_S - N_S|N_S\rangle\langle N_S|. \tag{4}$$

The system Hamiltonian is then defined as $H_S = \omega_S(a_S^\dagger a_S + 1/2)$; in the following we set $\hbar = 1$ and express all frequencies in units of ω_S. As discussed in Ref. 22, this definition turns out to be particularly convenient for numerical simulations and reproduces the expected dynamical behavior of truncated coherent states. These states are best obtained[22,27] as truncated coherent superposition of Fock states given by the repeated action of the adjoint of the operator defined in Eq. (2). The validity of this strategy is illustrated in Fig. 1, where we show the time evolution of a truncated coherent state both for the ideal harmonic-oscillator dynamics and including damping effects due to environmental interaction, thus demonstrating that the truncation does not introduce spurious effects within the relevant time window. The environmental Hamiltonian H_E is constructed as a Hermitian random matrix with complex entries. The dimension of this random matrix is fixed to N_E, which sets the effective dimensionality of the environment. The same construction is used for X_E. The choice of the relative sizes of N_S and N_E is optimized so as to ensure numerical feasibility while at the same time allowing the environment to induce the relevant effects on the system dynamics. The matrices H_E and X_E are independently sampled from the Gaussian unitary ensemble, rescaled by a factor $1/\sqrt{N_E}$ to compensate for the scaling of the eigenvalues with the environmental dimension.[28]

In contrast to Ref. 22, the environment in this work is initially in a mixed state. This necessitated the use of the density matrix formalism from the outset, significantly increasing the computational time. In this regard, our simulations were performed with a system dimension $N_S = 16$ and an environment dimension $N_E = 64$. These parameters allowed us to ensure that the norm deviation of the truncated

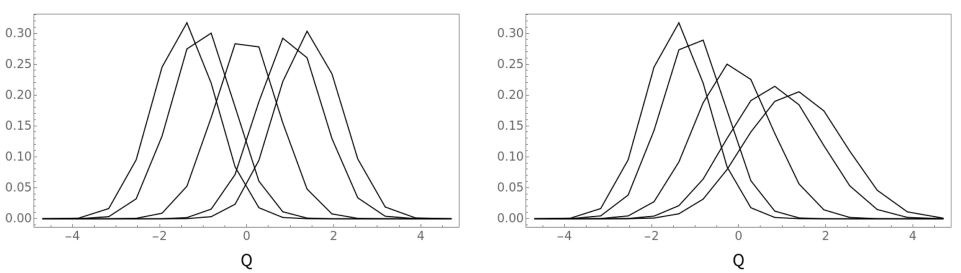

Fig. 1. Time evolution of a truncated coherent state for the free system Hamiltonian $H_S = \omega_S(a_S^\dagger a_S + 1/2)$ (left) and in the presence of damping due to a thermal environment with coupling strength $\gamma = 0.32$ and bath temperature (see Eq. (27)) $\theta = 0.1$ (right); both in units of ω_S. The plots show the squared modulus of the wave-function as a function of position at different times, moving with time from left to right. These results benchmark the validity of the ACL model for the description of the reduced dynamics.

coherent states from the exact expression (obtained for the infinite-dimensional case) was limited to 10^{-7} for a displacement $\alpha = 1$.

3. Non-Markovian Dynamics and Information Backflow

Broadly speaking, the dynamics of an open system is Markovian when memory effects induced by the interaction with the environment can be neglected.[1] Starting from this and motivated by the analogous notion in classical stochastic processes,[29] Markovianity has been extended to the quantum domain in several, generally nonequivalent, definitions.[15,17,19,30] In particular, one can rely on a rigorous and physically transparent way to identify memory effects with a bidirectional exchange of information between the open system and the environment. In this picture, information flows first from the system to the environment, and subsequently in the opposite direction, so that information about the system's state at earlier times influences its evolution at later times. First formulated by using the trace-distance revivals as indicators of information backflow,[20] this approach has then been generalized to include different quantifiers that, as the trace distance, evaluate the distinguishability between quantum states, so that a backflow of information manifests as an increase in the states' distinguishability.[31–34]

After introducing the general properties needed to identify quantum states' distinguishability quantifiers, we will here briefly recall how the latter can be used to define and quantify non-Markovianity for open quantum system dynamics. We will further present a general bound to their revivals, which clarifies the role of system-environment correlations and changes in the environmental state in establishing information backflow.

3.1. *Distinguishability quantifiers*

Let $\mathfrak{S}(\rho^{(1)}, \rho^{(2)})$ be any quantity defined on any couple of quantum states $(\rho^{(1)}, \rho^{(2)})$, i.e. Hermitian, positive operators with trace one, that satisfies the following properties: (i) it is nonnegative, bounded and normalized, according to

$$0 \leq \mathfrak{S}(\rho^{(1)}, \rho^{(2)}) \leq 1 \quad \forall \rho^{(1)}, \rho^{(2)}, \tag{5}$$

with

$$\mathfrak{S}(\rho^{(1)}, \rho^{(2)}) = 1 \Leftrightarrow \rho^{(1)} \perp_{\text{supp}} \rho^{(2)}, \tag{6}$$

where $\perp_{\text{supp}}$ denotes orthogonal supports, and

$$\mathfrak{S}(\rho^{(1)}, \rho^{(2)}) = 0 \Leftrightarrow \rho^{(1)} = \rho^{(2)}; \tag{7}$$

(ii) it is contractive under completely positive trace preserving (CPTP) maps:

$$\mathfrak{S}(\Lambda[\rho^{(1)}], \Lambda[\rho^{(2)}]) \leq \mathfrak{S}(\rho^{(1)}, \rho^{(2)}) \quad \forall \rho^{(1)}, \rho^{(2)}, \ \forall \text{CPTP } \Lambda; \tag{8}$$

(iii) it satisfies the triangular inequalities

$$\mathfrak{S}(\rho^{(1)},\rho^{(2)}) - \mathfrak{S}(\rho^{(1)},\rho^{(3)}) \leq \mathfrak{S}(\rho^{(2)},\rho^{(3)}) \quad \forall \rho^{(1)},\rho^{(2)},\rho^{(3)},$$
$$\mathfrak{S}(\rho^{(2)},\rho^{(1)}) - \mathfrak{S}(\rho^{(3)},\rho^{(1)}) \leq \mathfrak{S}(\rho^{(2)},\rho^{(3)}) \quad \forall \rho^{(1)},\rho^{(2)},\rho^{(3)}. \tag{9}$$

These are the requirements we ask for a quantity to be a proper quantifier of the distinguishability between quantum states. In fact, property (i) ensures that distinguishability is a nonnegative number, it is normalized to 1 (which is useful when comparing different quantifiers), as well as that only and all identical states are indistinguishable and that maximal distinguishability is achieved for only and all states that can be discriminated in single-shot measurements. Property (ii), which can be seen as an instance of the quantum data-processing inequality,[35] expresses that distinguishability cannot be increased by any operation on a quantum system, such as a measurement or an evolution induced by the interaction with a second, initially uncorrelated system in a fixed state. Finally, property (iii) is the crucial ingredient to relate the changes in the states' distinguishability of a quantum system with the information contained within other degrees of freedom; note that it can be relaxed to a weaker requirement, while keeping the same physical picture presented in the next subsections.[34]

Contractivity under CPTP maps is arguably the most relevant requirement for a quantifier of quantum states' distinguishability, both because of its physical meaning and because it implies other relevant features. In particular, Eq. (8) implies that the quantifier is invariant under unitary transformations

$$\mathfrak{S}(U\rho^{(1)}U^\dagger, U\rho^{(2)}U^\dagger) = \mathfrak{S}(\rho^{(1)},\rho^{(2)}) \quad \forall \rho^{(1)},\rho^{(2)}, \quad \forall \text{ unitary } U, \tag{10}$$

as well as under the tensor product with a fixed state,

$$\mathfrak{S}(\rho^{(1)},\rho^{(2)}) = \mathfrak{S}(\rho^{(1)}\otimes\rho^{(3)},\rho^{(2)}\otimes\rho^{(3)}) \quad \forall \rho^{(1)},\rho^{(2)},\rho^{(3)}, \tag{11}$$

and it further leads to the orthogonality of only and all the pairs of states maximizing the quantifier, provided that the invariance of the latter guarantees sufficiency of the map[36] when restricted to commuting states.[37]

Two significant examples, which we will use in the following analysis, are given by the trace distance $D(\rho^{(1)},\rho^{(2)})$ and the square root of the Jensen–Shannon divergence $\sqrt{\mathrm{J}(\rho^{(1)},\rho^{(2)})}$. The former is defined as one half the trace norm of the difference between the two quantum states it refers to:

$$D(\rho^{(1)},\rho^{(2)}) = \frac{1}{2}\|\rho^{(1)}-\rho^{(2)}\|_1 = \frac{1}{2}\sum_i |\ell_i|, \tag{12}$$

where $\|\cdot\|_1$ is the 1−norm, so that the ℓ_is are the eigenvalues of the Hermitian traceless operator $\rho^{(1)}-\rho^{(2)}$, and it then naturally satisfies the properties (i)–(iii). Given the quantum relative entropy[38]

$$S(\rho,\sigma) = \mathrm{tr}\{\rho\log\rho\} - \mathrm{tr}\{\rho\log\sigma\}, \tag{13}$$

the Jensen–Shannon divergence is defined as[3,38]

$$\mathsf{J}(\rho^{(1)},\rho^{(2)}) = \frac{1}{2\log 2}\left(S\left(\rho^{(1)},\frac{\rho^{(1)}+\rho^{(2)}}{2}\right)+S\left(\rho^{(2)},\frac{\rho^{(1)}+\rho^{(2)}}{2}\right)\right), \quad (14)$$

and it satisfies property (i) and (ii), which are then shared by its square root $\sqrt{\mathsf{J}(\rho^{(1)},\rho^{(2)})}$; not only, but the latter is a distance,[39,40] so that it also satisfies property (iii).

3.2. *Non-Markovianity measure*

Having introduced the notion of quantum-state distinguishability quantifier $\mathfrak{S}(\rho^{(1)},\rho^{(2)})$, we now show how this allows one to define and quantify non-Markovianity for general open quantum system dynamics.

Hence, consider the open system S and the environment E, which are uncorrelated at the initial time $t_0 = 0$,

$$\rho_{SE}(0) = \rho_S(0)\otimes\rho_E(0), \quad (15)$$

where $\rho_E(0)$ is a fixed environmental state, and which form together a closed system evolving unitarily, as fixed by the group of unitary operators $U(t)$. Then, the reduced evolution of the open system is described by a one-parameter family of CPTP maps $\{\Lambda(t)\}_{t\geq 0}$, according to[1]

$$\rho_S(t) = \Lambda(t)[\rho_S(0)] = \mathrm{tr}_E\{U(t)(\rho_S(0)\otimes\rho_E(0))U^\dagger(t)\}, \quad (16)$$

with tr_E the partial trace over the environment. Given two initial conditions, $\rho^{(1)}_{SE}(0) = \rho^{(1)}_S(0)\otimes\rho_E(0)$ and $\rho^{(2)}_{SE}(0) = \rho^{(2)}_S(0)\otimes\rho_E(0)$, so that $\rho^{(i)}_S(t) = \Lambda(t)[\rho^{(i)}_S(0)]$ for $i = 1, 2$, and instants of time s and $t \geq s$, the difference

$$\Delta_S\mathfrak{S}(t,s) = \mathfrak{S}(\rho^{(1)}_S(t),\rho^{(2)}_S(t)) - \mathfrak{S}(\rho^{(1)}_S(s),\rho^{(2)}_S(s)) \quad (17)$$

tells us the change of the quantum states' distinguishability from time s to time t, as quantified by $\mathfrak{S}$, under the evolution fixed by $\{\Lambda\}_{t\geq 0}$.

Now, the basic idea is that a decrease in distinguishability is associated with information flowing out of the open system, thus leading to a reduction of the ability to discriminate among the two initial conditions $\rho^{(1)}_S(0)$ and $\rho^{(2)}_S(0)$, while an increase in distinguishability means that some information is flowing into the open system. The sequence of two time intervals $[t_1,t_2]$ and $[t_2,t_3]$ such that a distinguishability decrease, $\Delta_S\mathfrak{S}(t_2,t_1) < 0$, is followed by an increase, $\Delta_S\mathfrak{S}(t_3,t_2) > 0$, is then interpreted as a bidirectional flow of information: some of the information about the initial condition that left the open system during $[t_1,t_2]$ is recovered by it during $[t_2,t_3]$. Such a recovery of information is the essence of the notion of memory effect, and it can thus be used to define (non-)Markovianity in open system dynamics. Explicitly, we say that the open-system dynamics $\{\Lambda(t)\}_{t\geq 0}$ is Markovian when

the rate

$$\sigma(\rho_S^{(1)}(0), \rho_S^{(2)}(0), t) = \frac{d}{dt}\mathfrak{S}(\rho_S^{(1)}(t), \rho_S^{(2)}(t)) \tag{18}$$

is nonpositive for every time and couple of initial states:

$$\sigma(\rho_S^{(1)}(0), \rho_S^{(2)}(0), t) \leq 0 \quad \forall\, \rho_S^{(1)}(0), \rho_S^{(2)}(0), t. \tag{19}$$

Markovian dynamics are those characterized by a unidirectional flow of information out of the open system: any information leaving it is irreversibly lost and cannot affect the open system dynamics back again. Conversely, non-Markovian dynamics are those where there is at least a couple of initial conditions and a time interval for which some information flows back to the open system, i.e. such that $\Delta_S\mathfrak{S}(t, s) > 0$ on that interval and then $\sigma(\rho_S^{(1)}(0), \rho_S^{(2)}(0), \tau) > 0$ for some $\tau \in [s, t]$.

Not only does this approach allow for a clear-cut definition of quantum Markovianity, but it also provides a natural way to quantify non-Markovianity. The first step to do so is to integrate over all the increases of distinguishability, i.e. over all the information about the initial conditions that flows back to the open system in the course of the evolution, thus getting

$$\mathcal{N}(\rho_S^{(1)}(0), \rho_S^{(2)}(0)) = \int_{\sigma>0} dt\, \sigma(\rho_S^{(1)}(0), \rho_S^{(2)}(0), t). \tag{20}$$

By further maximizing over all couples of initial conditions,

$$\mathcal{N}_{\Lambda(t)} = \max_{(\rho_S^{(1)}(0), \rho_S^{(2)}(0))} \int_{\sigma>0} dt\, \sigma(\rho_S^{(1)}(0), \rho_S^{(2)}(0), t), \tag{21}$$

we are left with a quantity that is associated with the family of CPTP maps fixing the dynamics of the open system (as stressed by the subscript $\Lambda(t)$), without depending on a specific choice of the initial conditions. Note that, at least for some distinguishability quantifiers including the trace distance, the evaluation of the maximum in Eq. (21) can be strongly simplified by general results,[32,41,42] implying in particular that the optimal pair is always given by two orthogonal states on the boundary of the state space.

3.3. *Bounds on system-environment information exchange*

The physical picture based on the notion of information flow can be further substantiated by taking into account the dynamical evolution of the information, not only inside the open system, but also outside it and then at the global level.

Let thus (where for the sake of readability we leave the dependence on $(\rho_S^{(1)}(0), \rho_S^{(2)}(0))$ implied)

$$\mathcal{I}_{\text{int}}(t) = \mathfrak{S}(\rho_S^{(1)}(t), \rho_S^{(2)}(t)) \tag{22}$$

be the amount of information within the open system, i.e. that can be accessed via measurements on S only, and

$$\mathcal{I}_{\rm ext}(t) = \mathfrak{S}(\rho_{SE}^{(1)}(t), \rho_{SE}^{(2)}(t)) - \mathfrak{S}(\rho_{S}^{(1)}(t), \rho_{S}^{(2)}(t)) \tag{23}$$

the amount of information outside it. The factorized initial condition and Eq. (11) imply

$$\mathfrak{S}(\rho_{SE}^{(1)}(0), \rho_{SE}^{(2)}(0)) = \mathfrak{S}(\rho_{S}^{(1)}(0), \rho_{S}^{(2)}(0)),$$

so that $\mathcal{I}_{\rm ext}(0) = 0$: since the global initial condition is a factorized state, with a fixed state of the environment, all the initial information about it is contained within the open system. Moreover, the global unitary evolution does not modify the total amount of information, i.e. Eq. (10) implies

$$\mathfrak{S}(\rho_{SE}^{(1)}(t), \rho_{SE}^{(2)}(t)) = \mathfrak{S}(\rho_{SE}^{(1)}(0), \rho_{SE}^{(2)}(0)),$$

so that all in all we have

$$I_{\rm int}(t) + I_{\rm ext}(t) = I_{\rm int}(0). \tag{24}$$

The information about the initial condition, initially only within the open system, is then exchanged between the open system and the environment, so that any backflow of information to the open system in the time interval $[s, t]$ corresponds to a decrease of the external information that has been collected up to time s. By using properties (ii) and (iii), one can upper bound the distinguishability increase due to a backflow of information, according to

$$\begin{aligned}\Delta_S \mathfrak{S}(t, s) \leq I_{\rm ext}(s) \leq\ & \mathfrak{S}(\rho_{SE}^{(1)}(s), \rho_{S}^{(1)}(s) \otimes \rho_{E}^{(1)}(s)) \\ & + \mathfrak{S}(\rho_{SE}^{(2)}(s), \rho_{S}^{(2)}(s) \otimes \rho_{E}^{(2)}(s)) + \mathfrak{S}(\rho_{E}^{(1)}(s), \rho_{E}^{(2)}(s)).\end{aligned} \tag{25}$$

This bound provides us with a general characterization of the microscopic mechanisms behind the occurrence of memory effects, extending the corresponding physical picture for the trace distance[17,43–49] to general distinguishability quantifiers.[34] The amount of states' distinguishability that can be recovered in a certain time interval $[s, t]$ is upper bounded by the information that is outside the open system at time s. Such external information is in turn bounded by the sum of the total correlations, both classical and quantum, that are present in the two global states that evolve from the initial conditions to time s, and the distinguishability in the corresponding environmental states. Indeed, the external information is contained not only within the environment, but also in the system-environment correlations. Conversely, Eq. (25) implies that any backflow of information is induced by the correlations established between the system and the environment, and by the information stored in the environment.

Of course, different distinguishability quantifiers $\mathfrak{S}(\rho_S^{(1)}, \rho_S^{(2)})$ will generally lead to different degrees of non-Markovianity, possibly even to a different classification of Markovian and non-Markovian dynamics, as well as to a different quantification of the system-environment correlations and changes in the environmental states; the

comparison among two relevant quantifiers is indeed a central subject of our investigation. On the other hand, we remark that the physical picture now illustrated does hold irrespectively of the considered quantifier.

4. Results

We are now ready to present the results of our investigation, namely, the assessment of the degree of non-Markovianity and its connection with the system-environment correlations and changes in the environmental states for the ACL model.

4.1. *Time-evolution of the distinguishability quantifiers*

As explained in Sec. 3.2, the notion of non-Markovianity investigated in this work is based on the time evolution of state distinguishability, obtained by comparing the dynamics arising from two distinct initial open-system states, assuming initial global product states as in Eq. (15). Throughout our analysis, we fix the initial system states as the truncated coherent states

$$\rho_S^{(1)}(0) = |\alpha\rangle\langle\alpha|\,, \quad \rho_S^{(2)}(0) = |-\alpha\rangle\langle-\alpha|\,, \tag{26}$$

defined as detailed in Sec. 2.1, considering $\alpha = 1$, while the environment is taken to be initially in a Gibbs state at temperature θ (we set $k_B = 1$)

$$\rho_E(0) = \frac{e^{-H_E/\theta}}{Z}, \qquad Z = \mathrm{tr}\{e^{-H_E/\theta}\}. \tag{27}$$

In Fig. 2, we show the time evolution of two distinguishability quantifiers: the trace distance, $\mathfrak{S}(\rho_S^{(1)}(t), \rho_S^{(2)}(t)) \mapsto D(\rho_S^{(1)}(t), \rho_S^{(2)}(t))$ (left panel), and the square root of the Jensen–Shannon divergence, $\mathfrak{S}(\rho_S^{(1)}(t), \rho_S^{(2)}(t)) \mapsto \sqrt{\mathrm{J}(\rho_S^{(1)}(t), \rho_S^{(2)}(t))}$ (right panel), as functions of time, for different values of the system-environment coupling strength γ and fixed environmental temperature θ. For both quantifiers and across the entire parameter regime considered, we observe clear nonmonotonic time evolutions, indicating the widespread presence of memory effects in the

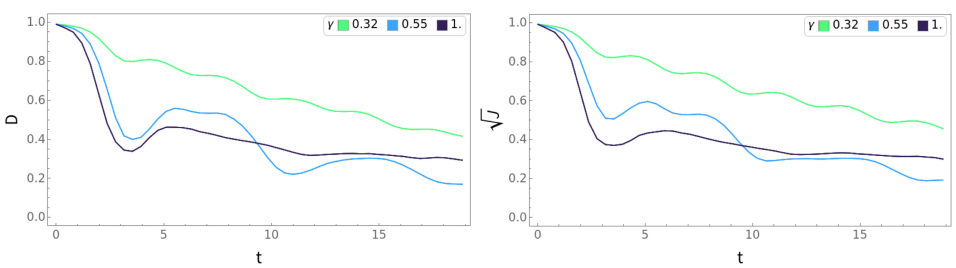

Fig. 2. Trace distance $D(\rho_S^{(1)}(t), \rho_S^{(2)}(t))$ (left) and square root of the Jensen–Shannon divergence $\sqrt{\mathrm{J}(\rho^{(1)}(t), \rho^{(2)}(t))}$ (right) as a function of time, for different values of the coupling γ, at fixed bath temperature $\theta = 1$; the two initial open-system states are as in Eq. (26) for $\alpha = 1$.

model. For a small coupling, the dynamics exhibits repeated oscillations with relatively small amplitudes, corresponding to modest but persistent revivals of distinguishability over the full time window taken into account. As the coupling strength increases, more pronounced revivals appear, but which now tend to concentrate into two distinct time intervals. Moreover, we note that the first dip of quantum states' distinguishability and subsequent revival is more pronounced as quantified by the trace distance compared to the square root of the Jensen–Shannon divergence. For the strongest coupling, the first revival is further amplified, while the second one is almost completely suppressed. This behavior reflects a competition between short-time information backflow, which is strengthened by increasing the coupling, and an accelerated relaxation toward a (quasi-)[a] steady state, in which oscillations are largely diminished.

4.2. *Degree of non-Markovianity*

We now move to the quantifier of the degree of non-Markovianity $\mathcal{N}$ defined in Eq. (20) (implying the dependence on the two initial conditions in Eq. (26)). By integrating the revivals of distinguishability, $\mathcal{N}$ provides a cumulative assessment of the information backflow, and thus of the memory effects over the entire evolution. This allows us to compare different dynamical scenarios, such as the presence of many small revivals distributed over time versus a smaller number of more pronounced revivals. We focus on a fixed pair of initial states and therefore evaluate $\mathcal{N}$, rather than the fully optimized non-Markovianity measure $\mathcal{N}_{\Lambda(t)}$ defined in Eq. (21), since the latter would require an optimization over initial states that is computationally prohibitive given the high dimensionality of the open system; in any case, $\mathcal{N}$ provides a lower bound to $\mathcal{N}_{\Lambda(t)}$. In our numerical analysis, the integral in Eq. (20) is evaluated up to a fixed finite maximum time, for all parameters considered. Furthermore, the integral is computed using a discretized time grid; we verified convergence by varying the time step Δt and confirming that doubling it leads to no appreciable change in the resulting value of the quantifier. We report results only for the trace distance, since those obtained using the square root of the Jensen–Shannon divergence are qualitatively and largely quantitatively similar.

In Fig. 3, we show the behavior of $\mathcal{N}$ as a function of the coupling strength γ for different values of the temperature θ (left panel), and as a function of θ for different values of γ (right panel). As a function of the coupling, non-Markovianity displays a nonmonotonic behavior, reflecting the competition between the physical mechanisms discussed above. Increasing the coupling from the small- to the intermediate-coupling regime enhances the exchange of information between the open system and the environment over the entire evolution, while further moving to stronger couplings the accelerated relaxation toward equilibrium prevails: distinguishability oscillations are progressively suppressed, and eventually the entire

[a]Since the global system considered is finite-dimensional, the open-system state does not converge asymptotically to a stationary state, but recurrences occur on sufficiently long time scales.[50]

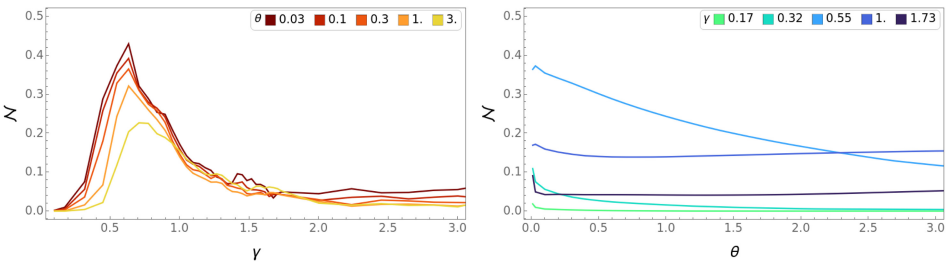

Fig. 3. Non-Markovianity $\mathcal{N}$ as defined in Eq. (20) for the two initial states in Eq. (26) with the trace distance as distinguishability quantifier, as a function of the coupling γ for different values of θ (left) and as a function of the temperature θ for different values of γ (right).

backflow of information, as quantified by $\mathcal{N}$, is significantly reduced. Increasing the temperature θ lowers the maximum value of $\mathcal{N}$ as a function of γ, while shifting its position toward larger values of γ, and for strong couplings θ has a limited impact on $\mathcal{N}$.

We stress that both the nonmonotonic dependence of $\mathcal{N}$ on γ, with a maximum in the intermediate-coupling regime, and the tendency toward a temperature-independent behavior at strong coupling are also observed in the non-Markovianity measure of the standard Caldeira–Leggett model studied in Ref. 51, where the Bures distance was employed to quantify distinguishability. Beyond confirming the robustness of the information-backflow approach to non-Markovianity with respect to the specific choice of distinguishability quantifier, this agreement supports the ability of the ACL model to capture the essential physical features of quantum Brownian motion, also for what non-Markovianity is concerned.

This conclusion is further corroborated by looking at the dependence of $\mathcal{N}$ on the temperature θ. As for the Caldeira–Leggett model,[51] the low-temperature regime is that showing the highest degree of non-Markovianity, even though, for certain values of the coupling strength, zero temperature does not correspond to the absolute maximum of $\mathcal{N}$, but a weak nonmonotonic dependence on θ can be observed. Differently from the Caldeira–Leggett model, instead, we see that strongly increasing the temperature can actually enhance non-Markovianity, for large values of the coupling. We attribute this behavior to the finite size of the environment considered here: higher bath temperatures lead to a stronger impact of the truncation procedure described in Sec. 2.1 due to the larger occupation of the highest levels taken into account, which turns into finite-size effects amplifying memory effects.

4.3. *Role of system-environment correlations and environmental evolution in information backflow*

While the analysis of quantifiers such as $\mathcal{N}$ provides a characterization of the non-Markovianity of the reduced open-system dynamics, identifying the microscopic origin of such non-Markovianity requires examining the time evolution of global

quantities, accounting for the dynamics within the environment and the buildup of system-environment correlations induced by the interaction. The bound in Eq. (25) enables precisely this investigation, by linking revivals in the distinguishability of open-system states to the establishment of total correlations and to changes in the environmental state, all expressed in terms of the same distinguishability quantifier $\mathfrak{S}(\rho^{(1)}, \rho^{(2)})$.

In the left panels of Fig. 4, we report the time evolution of the total correlations, $D(\rho_{SE}^{(1)}(t), \rho_S^{(1)}(t) \otimes \rho_E^{(1)}(t))$, and of the distinguishability in the environmental states $D(\rho_E^{(1)}(t), \rho_E^{(2)}(t))$, both quantified using the trace distance, for different values of the coupling strength γ and the temperature θ; for the choice of initial conditions in Eq. (26), the dynamics of the total correlations of $\rho_{SE}^{(1)}(t)$ and $\rho_{SE}^{(2)}(t)$ coincide. The interaction progressively establishes system-environment correlations, which build up more rapidly and reach larger values for stronger coupling

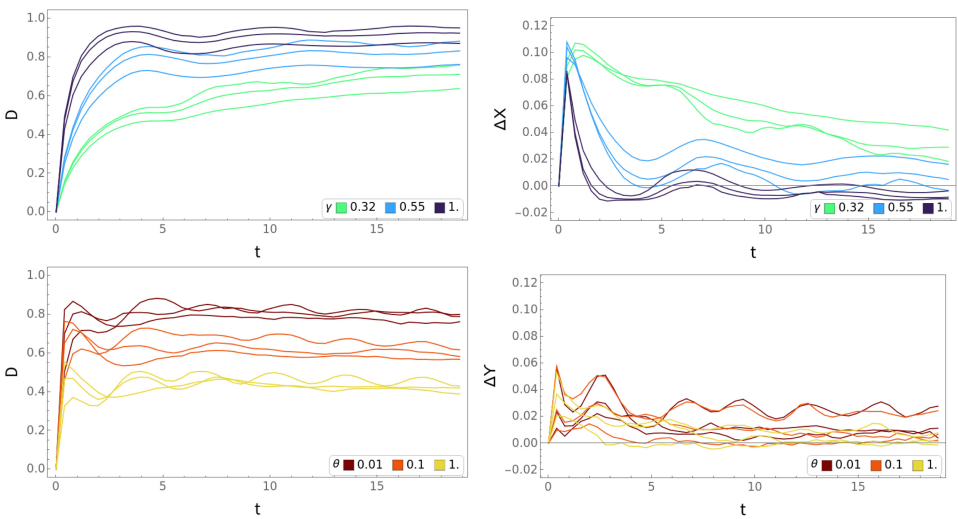

Fig. 4. (Left panels) Trace-distance system-environment correlations $D(\rho_{SE}^{(1)}(t), \rho_S^{(1)}(t) \otimes \rho_E^{(1)}(t))$ (upper panel) and changes in the environmental state $D(\rho_E^{(1)}(t), \rho_E^{(2)}(t))$ (lower panel) as a function of time, for different values of coupling and temperature $\gamma = \{0.32, 0.55, 1\}$; $\theta = \{0.01, 0.1, 1\}$; the other parameters are as in Fig. 3. (Right panels) Difference between the system-environment correlations evaluated with the square root of the Jensen–Shannon divergence and those evaluated via the trace distance, $\Delta X = \sqrt{\mathsf{J}(\rho_{SE}^{(1)}(t), \rho_S^{(1)}(t) \otimes \rho_E^{(1)}(t))} - D(\rho_{SE}^{(1)}(t), \rho_S^{(1)}(t) \otimes \rho_E^{(1)}(t))$, (upper panel) and difference between the changes in the environmental states with the two quantifiers, $\Delta\Upsilon = \sqrt{\mathsf{J}(\rho_E^{(1)}(t), \rho_E^{(2)}(t))} - D(\rho_E^{(1)}(t), \rho_E^{(2)}(t))$, (lower panel) for the same parameters as the left panels. In the upper panels, the different colors refer to distinct values of the coupling, while in the lower panels they refer to distinct values of the temperature; this reflects the larger impact of coupling and temperature variations on the evolution of, respectively, system-environment correlations and changes in the environmental state. In the upper panels, for a fixed coupling, the temperature increases moving from upper to lower lines (referring to the values at the first maximum), while in the lower, for a fixed temperature, the coupling increases moving from lower to upper lines. Note the difference in scale between the right and the left panels.

and lower temperature; indeed, variations in the coupling strength have a more pronounced effect on the evolution of global correlations than changes in temperature. We highlight these features in the left panels of Fig. 4 by using colors to emphasize the bunching of lines around the values of the physical parameters that most significantly affect each figure of merit: namely, the coupling strength for the correlations and the temperature for the environmental changes. Across all regimes considered, the total correlations tend to saturate at long times, as the system approaches a (quasi-)stationary state. Apart from modifying the speed at which the system-environment correlations are formed, both γ and θ have a relatively limited impact on their oscillations.

The distinguishability of environmental states quickly approaches a first peak, which also grows with γ and shrinks with θ, but where now the temperature has a more significant impact than the coupling strength. Interestingly, here we can observe a behavior that mirrors the competing mechanisms in the backflow of information discussed in the previous section: while increasing the coupling enhances the magnitude of changes in the environmental state, it also suppresses their oscillations at intermediate and long time scales.

Overall, the information outside the open-system leading to the backflow of information at the origin of non-Markovianity is shared by the system-environment correlations and the environmental state. The information within the latter is predominant at very short times, rapidly reaching a local maximum and then oscillating around it, whereas the information within correlations continues to grow throughout the dynamics, becoming prevalent at longer times. However, while correlations almost saturate to the maximal possible value, environmental changes have a smaller impact in absolute terms.

These behaviors are shared qualitatively and mostly quantitatively by the corresponding quantities, $\sqrt{\mathsf{J}(\rho_{SE}^{(1)}(t), \rho_{S}^{(1)}(t) \otimes \rho_{E}^{(1)}(t))}$ and $\sqrt{\mathsf{J}(\rho_{E}^{(1)}(t), \rho_{E}^{(2)}(t))}$, as evaluated via the square root of the Jensen–Shannon divergence. Therefore, in the right panel of Fig. 4 we report the difference between the Jensen–Shannon-based and trace-distance-based quantifiers of, respectively, system-environment correlations and environmental distinguishability. This difference is most pronounced at short times, where in particular for system-environment correlations it exhibits an initial peak that is almost independent of temperature and coupling strength, before decaying toward smaller values, with a faster decay for increasing coupling. A similar trend is observed for the difference between the environmental distinguishability quantifiers, although in this case the initial peak is less pronounced. We further note that, although the square root of the Jensen–Shannon divergence typically yields larger estimates than the trace distance, the differences for both system-environment correlations and environmental distinguishability can take on negative values, which demonstrates that no strict hierarchy exists between the two distinguishability quantifiers.

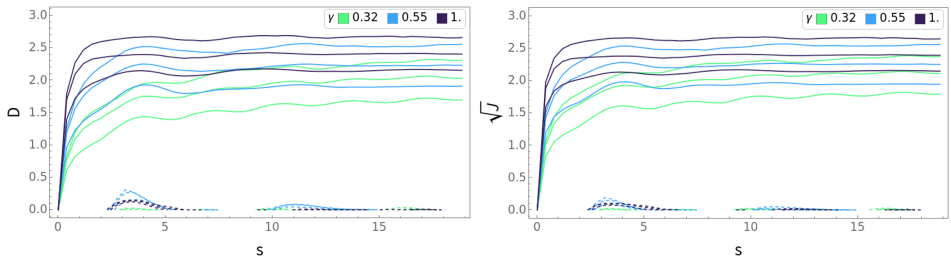

Fig. 5. System-environment correlations plus changes in the environmental state, i.e. right-hand side of the bound in Eq. (25), (solid lines) and variation of the open-system states' distinguishability, i.e. left-hand side of Eq. (25), (dashed lines) as a function of the intermediate time s, for the trace distance, $\mathfrak{S}(\rho^{(1)}, \rho^{(2)}) \mapsto D(\rho^{(1)}, \rho^{(2)})$ (left panel), and the square root of the Jensen–Shannon divergence, $\mathfrak{S}(\rho^{(1)}, \rho^{(2)}) \mapsto \sqrt{\mathrm{J}(\rho^{(1)}, \rho^{(2)})}$ (right panel); for each s, the final time t for the variation of distinguishability is taken as the closest local maximum (see Fig. 2).

Finally, the combined behavior of system-environment correlations and changes in the environmental state, that is the right-hand side of the bound in Eq. (25), is shown in Fig. 5, along with the corresponding variation of the open-system states' distinguishability, that is the left-hand side of Eq. (25), evaluated using both the trace distance and the square root of the Jensen–Shannon divergence quantifiers. In both cases, even though the applicability of the bound given by the right-hand side of Eq. (25) for estimating the left-hand side is indeed limited, the bound is nevertheless able to qualitatively reproduce some features of the dynamics. In particular, the nonmonotonic dependence on the coupling strength is captured, at least for intermediate and high temperatures, as is the monotonic decrease with increasing temperature. We also note that the behavior of the right-hand side of Eq. (25) for the two distinguishability quantifiers is more similar than the behavior of the left-hand side: while the open-system states trace distance exhibits a more pronounced first revival than the square root of the Jensen–Shannon divergence (see the discussion at the end of Sec. 4.1), such a feature is essentially absent in the corresponding upper bounds. Again, we observe that the upper bounds for the two distinguishability quantifiers are qualitatively and mostly quantitatively similar, with the more significant differences localized in the short-time regime. Overall, these results are in agreement with previous findings in exactly solvable models, in which both quantifiers demonstrated very similar performance.[33,52,53] Notably, our analysis confirms a slightly higher sensitivity of the trace distance in detecting revivals of distinguishability.

5. Conclusions

In this paper, we have explored the validity of the ACL model in characterizing the non-Markovianity of the Caldeira–Leggett model, focusing specifically on the information backflow that is considered to be at the heart of non-Markovian behavior. By exploiting the ability of the ACL model to conveniently address both

system and environment degrees of freedom, we have evaluated the amount of correlations established between the system and its surroundings, alongside the modifications in the environmental state induced by the interaction.

These quantities allow us to investigate a quantitative upper bound for the revival of distinguishability between system states, which is used as a criterion to identify non-Markovian dynamics. Our results indicate that, while correlations are sensitive to the coupling strength and weakly dependent on the environmental temperature, the opposite holds true for changes in the environmental states, which are more heavily influenced by temperature. These estimates appear to be consistent regardless of the chosen distinguishability measure, as we ascertained by comparing the trace distance and the square root of the Jensen–Shannon divergence.

Our results confirm that the ACL model is a reliable and computationally efficient proxy for the Caldeira–Leggett dynamics, particularly for exploring the emergence of memory effects. By establishing a quantitative connection between system-environment correlations and information backflow, we provide a solid basis for the physical interpretation of non-Markovianity. Future work will test the generality of these findings across diverse environmental geometries, including discrete spin-environments, to further consolidate our understanding of quantum memory.

Acknowledgments

This work has been supported by the Italian Ministry of Research and Next Generation EU via the PRIN 2022 project Quantum Reservoir Computing (QuReCo) (contract n. 2022FEXLYB), and the NQSTI-Spoke1-BaC project QuSynKrono (contract n. PE00000023-QuSynKrono). We gratefully acknowledge the computing resources provided by AMiCO (`http://amico.mi.infn.it`), an opportunistic resource cluster operated by the IT service of the Physics Department of Universitá degli Studi and INFN Milano — Italy.

ORCID

Luciano Manara https://orcid.org/0000-0001-9477-9497
Andrea Smirne https://orcid.org/0000-0003-4698-9304
Bassano Vacchini https://orcid.org/0000-0002-7574-9951

References

1. H.-P. Breuer and F. Petruccione, *The Theory of Open Quantum Systems* (Oxford University Press, Oxford, 2002).
2. A. Rivas and S. F. Huelga, *Open Quantum Systems: An Introduction* (Springer, Berlin, 2012).
3. B. Vacchini, *Open Quantum Systems: Foundations and Theory* (Springer Nature Switzerland, Cham, 2024).
4. W. H. Zurek, *Nat. Phys.* **5** (2009) 181.

5. W. H. Zurek, *Decoherence and Quantum Darwinism: From Quantum Foundations to Classical Reality* (Cambridge University Press, Cambridge, 2025).
6. R. Horodecki, J. K. Korbicz and P. Horodecki, *Phys. Rev. A* **91** (2015) 032122.
7. E. Ryan, M. Paternostro and S. Campbell, *Phys. Lett. A* **416** (2021) 127675.
8. B. Çakmak, Ö. E. Müstecaplıoğlu, M. Paternostro, B. Vacchini and S. Campbell, *Entropy* **23** (2021) 995.
9. J. K. Korbicz, *Quantum* **5** (2021) 571.
10. E. Joos, H. D. Zeh, C. Kiefer, D. Giulini, J. Kupsch and I.-O. Stamatescu, *Decoherence and the Appearance of a Classical World in Quantum Theory*, 2nd edn. (Springer, Berlin, 2003).
11. M. Schlosshauer, *Decoherence and the Quantum-to-Classical Transition* (Springer-Verlag, Berlin, 2007).
12. W. H. Zurek, *Rev. Mod. Phys.* **75** (2003) 715.
13. K. Hornberger, Introduction to decoherence theory, in *Entanglement and Decoherence*, eds. A. Buchleitner, C. Viviescas and M. Tiersch, Lecture Notes in Physics (Springer, Berlin, 2009), pp. 221–276.
14. P. Strasberg, *SciPost Phys.* **15** (2023) 24.
15. A. Rivas, S. F. Huelga and M. B. Plenio, *Rep. Prog. Phys.* **77** (2014) 094001.
16. H.-P. Breuer, *J. Phys. B* **45** (2012) 154001.
17. H.-P. Breuer, E.-M. Laine, J. Piilo and B. Vacchini, *Rev. Mod. Phys.* **88** (2016) 021002.
18. I. de Vega and D. Alonso, *Rev. Mod. Phys.* **89** (2017) 015001.
19. L. Li, M. J. Hall and H. M. Wiseman, *Phys. Rep.* **759** (2018) 1.
20. H.-P. Breuer, E.-M. Laine and J. Piilo, *Phys. Rev. Lett.* **103** (2009) 210401.
21. A. O. Caldeira and A. J. Leggett, *Phys. Rev. Lett.* **46** (1981) 211.
22. A. Albrecht, R. Baunach and A. Arrasmith, *Phys. Rev. Res.* **5** (2023) 023187.
23. A. Albrecht, R. Baunach and A. Arrasmith, *Phys. Rev. D* **106** (2022) 123507.
24. A. Albrecht, *Entropy* **24**(3) (2022) 316.
25. A. O. Caldeira and A. J. Leggett, *Physica A* **121** (1983) 587.
26. A. O. Caldeira and A. J. Leggett, *Ann. Phys. (N.Y.)* **149** (1983) 374.
27. T. Opatrný, A. Miranowicz and J. Bajer, *J. Mod. Opt.* **43** (1996) 417.
28. G. Livan, M. Novaes and P. Vivo, *Introduction to Random Matrices*, SpringerBriefs in Mathematical Physics, Vol. 26 (Springer International Publishing, Cham, 2018).
29. W. Feller, *An Introduction to Probability Theory and Its Applications*, Vol. 2 (John Wiley & Sons, New York, 1971).
30. S. Milz and K. Modi, *PRX Quantum* **2** (2021) 030201.
31. R. Vasile, S. Maniscalco, M. G. A. Paris, H.-P. Breuer and J. Piilo, *Phys. Rev. A* **84** (2011) 052118.
32. S. Wißmann, H.-P. Breuer and B. Vacchini, *Phys. Rev. A* **92** (2015) 042108.
33. N. Megier, A. Smirne and B. Vacchini, *Phys. Rev. Lett.* **127** (2021) 030401.
34. A. Smirne, N. Megier and B. Vacchini, *Phys. Rev. A* **106** (2022) 012205.
35. M. Nielsen and I. Chuang, *Quantum Computation and Quantum Information* (Cambridge University Press, Cambridge, 2000).
36. A. Jenčová, *Rev. Math. Phys.* **24** (2012) 1250016.
37. B. Vacchini, A. Smirne and N. Megier, Classical pair of states as optimal pair for quantum distinguishability quantifiers (2025) arXiv:2506.02575 [quant-ph] https://doi.org/10.48550/arXiv.2506.02575.
38. I. Bengtsson and K. Życzkowski, *Geometry of Quantum States: An Introduction to Quantum Entanglement*, 2nd edn. (Cambridge University Press, 2017).
39. D. Virosztek, *Adv. Math.* **380** (2021) 107595.
40. S. Sra, *Linear Algebra Appl.* **616** (2021) 125.

41. S. Wißmann, A. Karlsson, E.-M. Laine, J. Piilo and H.-P. Breuer, *Phys. Rev. A* **86** (2012) 062108.
42. B.-H. Liu, S. Wißmann, X.-M. Hu, C. Zhang, Y.-F. Huang, C.-F. Li, G.-C. Guo, A. Karlsson, J. Piilo and H.-P. Breuer, *Sci. Rep.* **4** (2014) 6327.
43. E.-M. Laine, J. Piilo and H.-P. Breuer, *Phys. Rev. A* **81** (2010) 062115.
44. A. Smirne, D. Brivio, S. Cialdi, B. Vacchini and M. G. A. Paris, *Phys. Rev. A* **84** (2011) 032112.
45. L. Mazzola, C. A. Rodríguez-Rosario, K. Modi and M. Paternostro, *Phys. Rev. A* **86** (2012) 010102.
46. A. Smirne, L. Mazzola, M. Paternostro and B. Vacchini, *Phys. Rev. A* **87** (2013) 052129.
47. E.-M. Laine, J. Piilo and H.-P. Breuer, *EPL* **92** (2010) 60010.
48. S. Campbell, M. Popovic, D. Tamascelli and B. Vacchini, *New J. Phys.* **21** (2019) 053036.
49. G. Amato, H.-P. Breuer and B. Vacchini, *Phys. Rev. A* **98** (2018) 012120.
50. P. Bocchieri and A. Loinger, *Phys. Rev.* **107** (1957) 337.
51. S. Einsiedler, A. Ketterer and H.-P. Breuer, *Phys. Rev. A* **102** (2020) 022228.
52. N. Megier, A. Smirne, S. Campbell and B. Vacchini, *Entropy* **24** (2022) 304.
53. B. Vacchini, *Int. J. Quantum Inf.* **22** (2024) 2450007.